Adaptively Equalized Bandwidth Optimization Model using SCADA-DWWAN based Neural Network

[1]PRIYANKO RAJ MUDIAR, [2]KANDARPA KUMAR SARMA, [3]NIKOS MASTORAKIS
[1, 2] Department of Electronics & Communication Engineering Gauhati University, Guwahati, INDIA
[3]Technical University, Sofia, BULGARIA.

Abstract: Artificial training and learning algorithms, enhanced with semi-supervised or self-supervised feature extraction capacities, employ adaptive decision optimization models. These are often favored over complex deep learning algorithms for achieving better controllability and ease of observation, lower complexity in simulating, building or designing and virtual prototyping of automatic network resource management (ANRM) standards. An Adaptive Linear Neuron type Artificial Neural Network (ADALINE-ANN) which is based on multi-tapered machine learning approach has been simulated in a virtual Supervisory Control and Data Acquisition (SCADA) framework integrated with a Distributed Control System (SCADA/DCS-Net). The system has been virtually simulated considering an adaptively equalized learning and decision approach which utilizes Markov Trained-Steepest Gradient Descent (HMM-SGD) based machine learning model employing Kalman optimization. Affinity clustering is employed for spectrum sensing by extracting the Constellation Nyquist Bands from an M-Quadrature Amplitude Modulation (QAM) orthogonal signal undergoing AWGN and Rayleigh fading as well as co-channel interference (CCI), and ensemble analysis using Channel State-Space plots are used for optimal spectrum allocation in an Adaptive Orthogonal Frequency Division Multiple Access (Adaptive-OFDMA) layout. It has been done by implementing an adaptively equalized Automatic Repeat Request (ARQ) pipelining model which utilizes minimum least square error (MLSE) minimization model. The objective is to improve the bandwidth allocation and usage ensuring most minimum spectrum wastage or loss. Successive Interference Cancellation (SIC) has been implemented to minimize static buffer and interference loss. Thus, spectrum loss due to latency and jitter which occurs from bandwidth congestion is minimized by improving the network resource tracking and allocation. It results in improved and stable bandwidth equalization.

Keywords: 256-Quaternary Amplitude Modulation(256-QAM), ADALINE, Kalman-Least Mean Square Algorithm (Kalman-LMS), Kalman optimized Kernel Recursive Least Square Algorithm (Kalman-KRLS), Affinity Propagation Clustering (AP-Clustering), Maximum Correntropy, ANOVEE, Eigen-Plot, Fourier-Bessel Transform, Huang-Hilbert Transform, Hidden Markov Model (HMM), Steepest Gradient Descent (SGD), Adaptive Automatic Repeat Request (Hybrid-ARQ), Maximal Ratio Combination Channel Diversity (MRCD), Successive Interference Cancellation (SIC).

Received: May 24, 2021. Revised: July 6, 2022. Accepted: August 8, 2022. Published: September 19, 2022.

1. Introduction

Almost every installation of cognitive IEEE-802.X wireless communication standards [1] which are designed and implemented for Supervisory Control and Data Acquisition (SCADA) based Digital Wireless Wide Area Networks (SCADA-DWWAN) including Industrial Control Network standards (DCS-Net) suffer from both co-channel interference (CCI) as well as bandwidth congestion for most of the multiple user stations or multi-access orthogonal transceiver stations [1][16][12]. Undiversified relaying, manual discrepancies in the network resource management as well as channel equalization errors lead to congestion and latency in secondary channels [1], which causes disruption and biasing in the utilization of the primary channel bandwidth, leading to spectrum losses [16]. Full-duplex switched-mode transmissions [11][15] suffer the worst bandwidth discrepancy [1][15] which occurs due to relay-buffer losses, bandwidth congestion and latency [1][11][15]. Field studies [1][7] and simulation tests [16] show that 'proper sensing and allocation' of sub-band resources in the Physical layer, Data-Link layer as well as Network layer of the different 'secondary station users' in each of the multiple access primary channels (PHY,MAC,FTP) using 'cooperative' and 'adaptive' spectrum sensing and sharing is likely to help mitigate the spectrum deficiencies caused by congestion which will collaboratively enhance the stability and fidelity of the network system. Although conventional artificial intelligence based models including machine learning prototypes [1][16] as well as deep learning neural network prototypes [16] and numerous convolutional neural network prototypes [16] have been designed, proposed and virtually tested in real time simulations, yet static convergence errors as well as dynamic decision errors show high rates of false-alarm and heuristic lags especially ranging over high frequency operational bands (350Mhz - 480Mhz) [1][2]. Since industrial supervisory and control networks mostly focus and rely upon precise controllability as well as high observation accuracy, hence Artificial Neural Networks (ANN's) utilizing adaptive learning, training and decision models are potentially likely to provide reliable solutions [1][16]. In our study, we have tested two popular ADALINE (Adaptive Linear Neuron) [6][9][13] based neural network models for application in 'spectrum sensing' [5] as well as 'spectrum allocation' [12][15] which are operationally semi-

supervised, dynamic decision models and have been formulated and simulated in an IEEE-802.22x SCADA-DWWAN based virtual transmission environment [1]. A novel ***Hidden Markov*** type ***stochastic gradient*** based ***training*** model [3] has been infused upon the standard ***"Widrow-Hoff Learning Method"*** implemented over ***Steepest Gradient Descent / Ascent (or Delta-learning) Rule*** using tuned kernel widths [13], thereby providing ***high dynamic learning adaptability*** as well as ***improved convergence*** during ***semi-supervised regression***. To ensure good controllability and equalised error interpolation, two novel Kalman optimization models [6][9] have been implemented upon a Least Mean Square (LMS) based spectrum sensing neuron [5] as well as a Kernelized Recursive Least Square (KRLS) based spectrum decisive neuron [12][15]. An "affinity detection and clustering" based feature extraction approach [2][4] is utilized for the sensing "or extraction" of Sub-Band Nyquist clusters from a spatial Constellation sequence [10] carrying 8-bit / 256-Quaternary Amplitude Modulation signals over an orthogonal multiple access transmission channel [11][12][15]. Applying a maximally correlative entropy equalization [17][13] concept, or "maximum-correntropy" condition, an adaptive channel diversity [11][12][15] based relaying and pipelining model is implemented which trains and decides the sub-channel spectrum allocation margins (or "Shannon sub-bands") according to an Eigen-space MLSE (Minimum Least Square Estimation) minimization approach [8][17], known as "Perron-Frobenius" model [17]. Thus, channel detection is achieved by identifying the cumulative entropies as well as mass ensemble distributions (CMF) in terms of some frequency convolved Energy Spectrum Distributions (ESD) by sequentially identifying and approximating the envelope side-band levels using Fourier Bessel Transforms and Huang-Hilbert Transforms [14] upon the sequentially identified Nyquist clusters with our proposed Markov-ADALINE type KRLS Neuron. An adaptively equalized routing prototype employs an Automatic Repeat Request (ARQ) based switch [15][17][22] over an adaptive orthogonal frequency division multiple access (OFDMA) virtual channel [7][11][15] for dedicated downlink relaying by estimating and aggregating the Maximal Signal-to-Noise Ratio (SNR) for each orthogonal sub-user links with a proposed ANN approach [3] against the minimum Bit Error Ratio (BER) paths by normalizing and mixing the Maximal sub-channel SNR Gains [7][15] over each route using a Maximal Ratio Combination approach. A semi-supervised approach has been formulated and proposed by authors [11][12] by updating the cost transition vectors using some ergodic Lagrangian determinants. This concept is being virtually implemented by our proposed Steepest Gradient Ascent/Descent based Hidden Markov Determinants (or Liapunov State Minimization Determinants, "LSMD") with respect to the ergodically but asymmetrically distributed "Perron-Frobenius" Eigen State Space Reduction (Eigen-SSR) Model [3][17].

Finally, generic training and learning performances have been obtained, visualized and then virtually tested with reference to the overall improvement in bandwidth equalization [17][20] as well as spectrum sensing [8] over the entire multiple access transmission channel [1][15].

2. Proposed Work

In this work, we report the design of an ANN based spectrum sensing and allocation system designed for a virtual SCADA-DCS framework. The design considers an adaptive Automatic Repeat Request (ARQ) mechanism in support of an Adaptive OFDMA network layout, as depicted in the block diagram in Fig. 1. Furthermore, the system uses Successive Interference Cancellation (SCI) which provides improved interference cancellation for bandwidth optimization [12].

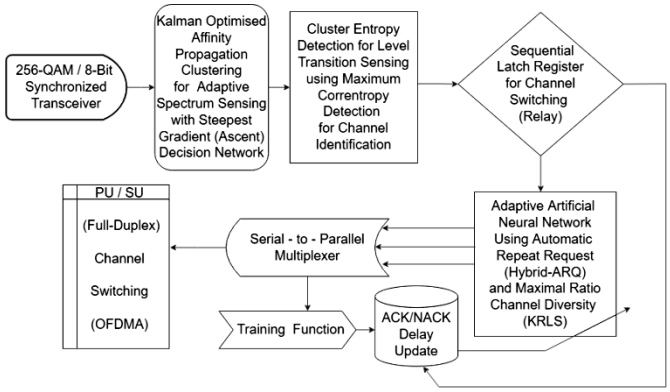

Fig. 1. *Block Diagram for Kalman-SGD/SGA ADALINE*

2.1 Spectrum Sensing

Constellation sequences which are obtained from a synchronous rake receiver channelling 8-bit octal words encoded over 256-Quaternary Amplitude Modulation (256-QAM) carrier signals are fed to a Kalman-optimized Least Mean Square ADALINE (LMSE) [6], to obtain the stochastic weights identifying each constellation cluster sequence using Steepest Gradient Descent rule (SGD), as shown in the block diagram in Fig. 1. A novel Hidden Markov training model [3] is implemented to optimize the sequencing and interpolation speeds as well as minimize the convergence errors while sampling the SGD training samples (or batches) for improvising the convergence speeds and regression efficiency of the SGD model. Thus, the 'Nyquist clusters' are identified and extracted from the constellation sequences by employing a novel Affinity Propagation [2][4] clustering method which detects the maximum availability measures (or maximum similarity measure between auto-correlation and auto-covariance) of each sequences between each constellation points [10] in order to identify and 'automatically link the constellation points' into 'groups' of separate sequential clusters or 'common correntropy symbols' carrying similar information, known as 'Nyquist-Bands'. By implementing an interpolative Fourier-Bessel Transform upon the identified and extracted Nyquist-clusters followed by Hilbert Transform using the novel Markov Trained SGD model under Gaussian Q-function limits, the gradient of the individual energy spectrum densities (ESD) or entropy transition levels corresponding to each of the 'ergodically identified' or 'sensed' clusters are being detected and are converged to identify the number of 'channel transitions' corresponding to each of the discrete energy levels in terms of cumulative mass function distribution (CMF). This detected ensemble

distribution corresponds to the aggregate Secondary User sub-bands against each Primary Channel User.

2.2 Spectrum Allocation

Corresponding to the CMF Levels, the signals extracted from each of the detected 256-clusters are being weighted by a Maximum Likelihood Sequence Estimator (MLSE) according to the individual aggregate ratios between Signal Power to Noise Power ratios (SNR) as well as Bit Error Rates (BER) for each 'identified' cluster [2][8][7]. Then, a clocked register phase-normalizes each of the serial cluster packets by co-phasing them (using a sequential clock synchronous phasing circuit) and feeding them serially to an ARQ assembly controlled by a Kernelized [9][13] Recursive Least Square (KRLS) ANN. Further, 20-virtual users comprising of 16-secondary users and 4-primary channel users have been implemented for parallel signal pipelining. The optimum transmission and reception capacity corresponding to each channel sub-user is determined using the delay information with respect to the maximal diversity ratios, or SNR gains mixed with minimum BER paths [7][15], which is identified and approximated from the envelope energies (ensemble entropies) by the Eigen-Space Minimization [17][8] model using HMM determinants [3], prior to each acknowledgement and non-acknowledgement key (ACK/NACK) [11][12]. Thus, using sequential/regressive training of the switching rates using a novel 'Lagrangian-Determinant' [12] for a Markov-trained Hybrid-ARQ [3][17], average Shannon Bands (sub-bands) are being determined corresponding to each primary/secondary station groups to achieve optimized sharing of the bandwidth while ensuring minimum buffer wastage as well as minimum critical latency. Hilbert frequency transforms [14] are used and learning curves are characterized for evaluating the performance and fidelity of our proposed architecture.

3. Proposed Methodology and Design

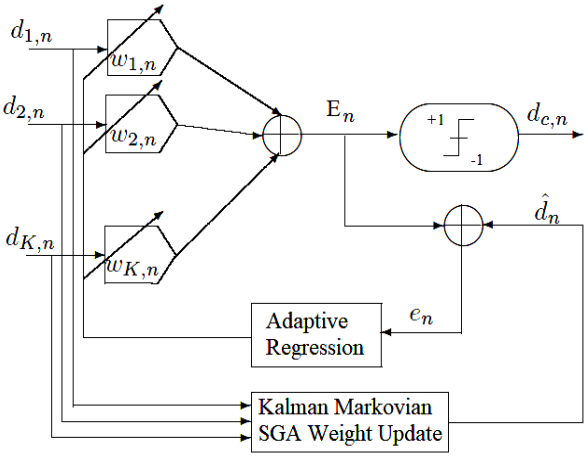

Fig. 2. *Generic logic flow model of ADALINE*

Let us consider the standard logic flow model of our proposed ADALINE Neuron as depicted in Fig.2.The Widrow-Hoff interpolation levels obtained for a parabolic sample signal implementing Steepest Gradient Descent (SGD) can be approximated as given in Fig.3. Let us consider the general MQAM signal entropy function as given by,-

$$\Phi_i(\tau) = \sqrt{\frac{2\epsilon}{Ts}} \cdot \left(a_i \cos\frac{2\pi t}{Ts} + b_i \sin\frac{2\pi t}{Ts}\right) \quad (1)$$

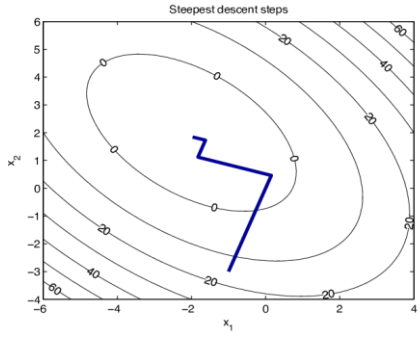

Fig. 3. *General pattern of Newtonian Interpolation for SGA/SGD*

Where, ϵ → *is the Minimum amplitude or lowest entropy signal and* (a_i , b_i) → *are the Eigen co-factors of any random signal constellation point* determined according to the respective coordinate location (Euclidean distance from each local centroids) . Let us consider a norm L = $\sqrt{M}$, for any M-coded Orthogonal QAM Signal (here, M = 256).

The local centroids corresponding to each individual constellation Nyquist Cluster can be determined with the i^{th} message points cardinally located as the binary tuple vector $(a_i\sqrt{\epsilon} , b_i\sqrt{\epsilon})$, where Eigen co-factors are an element of the $\{LxL\}$ matrix given by ,-

$$(a_i , b_i) = \begin{bmatrix} (-L+1, L-1) & (-L+3, L-1) & \dots (L-1, L-1) \\ (-L+1, L-3) & (-L+3, L-3) & \dots (L-1, L-3) \\ \vdots & \vdots & \vdots \\ (-L+1, -L+1) & (-L+3, -L+1) & \dots (L-1, -L+1) \end{bmatrix} \quad (2)$$

Let us consider the following typical S-T Windowed Constellation [16] , as shown in Fig. 4, standard for any M-QAM Signal undergoing AWGN Noise and Rayleigh Fading, given by authors [16], for (x_m, y_n) tuples , where $\boldsymbol{h = (x, y)}$ denotes the I/Q coordinates of the 256-QAM / 8-bit Signal , -

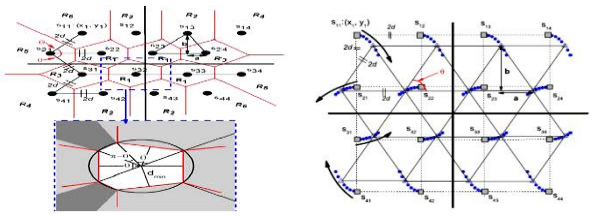

Fig. 4. *S/T Windowed Constellation for MQAM Signal [16]*

The constellation In-Phase / Quadrature (I/Q) coordinates can be expressed as given by authors [10] , -

$$(x_m , y_n) = [(2n-1) + 1 - \sqrt{M}\,].d + [2.mod(m , 2) - 1].(\tfrac{a}{2})$$
$$-[2(m-1) + 1 - \sqrt{M}\,].(\tfrac{b}{2}) \quad (3)$$

where , d → *is the cluster point Euclidean distance from local centroids; and* (m, n) → $[1, \dots\dots, \sqrt{\boldsymbol{M}}\,]$;

Thus, the similarity matrix, for each constellation point can be determined as [2][4]:

$$\Upsilon(m,n) = \left\| (x_m, x_n)^2 - (y_m, y_n)^2 \right\| \quad (4)$$

Let, tuple vector : $h_k = [h_k \quad h_{k-1} \quad h_{k-2} \quad h_{k-3} \quad ... \quad h_{k-N}]^T$

We know for LMS-SGD : $\widetilde{d_k(n)} = w^T_N(n) * h_N(n)$ (5)

$$\grave{e}_k(n) = h_k(n) - \widetilde{d_k(n)} \quad (6)$$

$$w_N(n+1) = w_N(n) - \alpha\, \grave{e}_k^*(n)\, h_N(n) \quad (7)$$

Where, $w_N \rightarrow$ *is the weight vector,* $\widetilde{d_k(n)} \rightarrow$ *is the equalizer learning output,* $\grave{e}_k(n) \rightarrow$ *is the iteration step error,* $h_k(n) \rightarrow$ *is the desired asymptote (local maxima of the SGD)* and $\alpha \rightarrow$ *is the convergence ratio or step size factor for an Ergodic distribution, and* $N \rightarrow$ *size of input constellation (m,n)*

The weight update function taken for normalized batches is,-

$$w_N(n+1) = w_N(n) - \frac{1}{2}\alpha \frac{\delta \grave{e}^2_k}{\delta w_N} = w_N(n) + \alpha\, \grave{e}_k(n) \frac{d^T_n}{d_n\, d^T_n} \quad (8)$$

Let $\sum_0^{2/\lambda}(x \sim n) \rightarrow$ denote the state covariance matrix of the weight transition vector, where $\lambda \rightarrow$ is the eigenvalue of the state covariance matrix and $R_{NN} \rightarrow$ denote the input correlation matrix. Convolving Kalman Filter rule in LMS / KRLS Widrow-Hoff Condition, we derive the posterior Kalman state space model as given below ,-

$$\alpha(n) = d_k(n) - h_k^T(n) \,.\, w_N \quad (9)$$

$$w_N(n+1) = \lambda w_N + \lambda \left[\frac{\sum_0^{2/\lambda}(x \sim n)\, h_k(n)\, \alpha(n)}{h_k^T(n) \sum_0^{2/\lambda}(x \sim n)\, h_k(n) + e_k(n)} \right] \quad (10)$$

$$\sum_0^{2/\lambda}(x \sim n+1) = \lambda^2 \sum_0^{2/\lambda}(x \sim n) - \dot{V}_k + \mu_k(n) \quad (11)$$

$$\dot{V}_k = \left[\frac{\lambda^2 \sum_0^{2/\lambda}(x \sim n)\, h_k(n)\, h_k(n)^T \,.\, \sum_0^{2/\lambda}(x \sim n)^H}{h_k^T(n) \sum_0^{2/\lambda}(x \sim n)\, h_k(n) + e_k(n)} \right] \quad (12)$$

$$\mu_k(n) = h_k^T(n).\ R_{kk}^{-1}(n-1).\ h_k(n) \quad (13)$$

To estimate the Affinity Correlation margins in order to iteratively determine the Minimum Entropy distances between each constellation propagation path, let us first derive the reduced correntropy determinants for Kalman-LMS/KRLS traced AP/SGD as we obtain the adaptive training state model,-

$$\ddot{\alpha}(n) = \Upsilon_k(n) \left[\frac{\partial \sum_0^{2/\lambda}(x \sim n)}{\partial \lambda} \right] - R_{kk}^{-1}(n-1)\, h_{k-1}(n).\, w_k(n) \quad (14)$$

$$[\sigma_w(n+1)]^2 = [\sigma_w(n)]^2 \left(1 - \frac{h_k(n)/N}{h_k(n) + e_k(n)/[\sigma_w(n)]^2}\right) + \mu_k \quad (15)$$

$$w_N(n+1) = w_N(n) + \frac{[d_k(n) * \ddot{\alpha}(n)] + \Upsilon_k}{h_k(n) + e_k(n)/[\sigma_w(n)]^2} \quad (16)$$

The recursive hyper-parameters or gradient interpolation determinants for affinity propagation clustering [4] to "extract" the constellation correntropy clusters for MQAM Const.^{n} are,-

Responsibility / Availability margins : $(r \overset{(*)}{\rightarrow} a)$, -

$$r^{(N)}(m,n) = (1-\beta)\Big(\Upsilon(m,n) - \max_{k \neq n} \{a(m,n) + \Upsilon(m,n)\} + \{\beta * r^{(N-1)}(m,n)\} \quad (17)$$

$$a^{(N)}(m,n) = \begin{cases} (1-\beta)\left(\min\left(0, r(m,n) + \sum_{k \neq \{m,n\}}^{N} \max(0, r(k,n))\right)\right) + \{\beta * a^{(N-1)}(m,n)\} \\ \quad if \ (m \neq n) \ ; \\ \quad or \\ (1-\beta) * \{\sum_{k \neq (n)}^{N} \max(0, r(k,n))\} + \{\beta * a^{(N-1)}(m,n)\} \\ \quad if \ (m = n) \ ; \end{cases}$$

Where, β :[0,1] $\rightarrow$ is the exponential damping fraction known as the ***"regression factor"***. Bigger values of (β) lowers the possibility of oscillation ***as well error*** in the iteration process, and also kernelizes the epoch points. Here, $r \rightarrow$ *denotes the responsibility margin* and $a \rightarrow$ *denotes the availability margin*.

The next step is to identify the ensemble densities (or Energy Spectrum Density) for each identified clusters in terms of their band distribution, and then determining their cumulative Gaussian entropy levels for channel estimation. In order to improve convergence speeds as well as dynamic efficiency, authors [3] have proposed and implemented a Markov Trained, Eigen-Space induction model upon the conventional Kalman-LMS approach in order to "dynamically reduce" the training batch sizes during each LMS iteration.

For an Ergodic model, Markov State model is given as [3], -

$$\theta_{k+1}^{(\Upsilon)} = \theta_k^{(\Upsilon)} - \Upsilon.[f'(\theta'_k{}^{(\Upsilon)}) + \eta_{k+1}.\, \theta_k^{(\Upsilon)}$$

$$\text{Provided,} \quad h_n = \kappa'_{k+1} \,.\, \theta_{k+1} + \grave{e}_k(n) \quad (18)$$

Where, $\eta \rightarrow$ is the regression factor ; $\kappa'_{k+1} \rightarrow$ is the state convergence factor, $\ddot{\alpha}(n)$ in HMM Model space. $\Upsilon \rightarrow$ *is the similarity determinant obtained by taking the Wronskian Determinant for each* R_{NN} .

For any epoch nodal point, along the principal trajectory, $\theta_k^{(\Upsilon)} : k \in (i, j \leq N)$, the Markovian STM (State Transition Model) is normally given as [3] ,-

$$\theta_{k+1}^{(\Upsilon)} = \frac{1}{k+1} \sum_{j=0}^{k} \theta_j \ (k)$$

Thus the Most Likelihood Estimator (MLE) for Markovian STM masked over any orthogonal signal is given [3] as,-

$$E_k(\theta_k - \theta_{k+1}) = \sum_{i=1}^{m} \left[\theta_{k+1} - \sum_{j=1}^{n} \theta_k \left\{ \frac{\kappa'_{k+1}}{\sigma_w(k)} \right\}^{\eta_{k+1}} \right] I_{\theta_k \leq \theta_i}$$

$$= \eta_{k+1} \sum_i^m \sum_j^n \theta_k\, \mu_k\, (i,j) = Q(\eta_{k+1})$$

To find the Eigen Space Model, authors [3] have provided Liapunov determinants to determine any general Minimization Model for Markovian MLSE Interpolation which can be used identically in place of Lagrangian Correctors [11][12][15] for predicting and correcting decision margins in terms of both LMS and KRLS Markovian approximation as given by ,-

$$\Gamma_1{}^{\kappa'_k}(\theta_k, n) = -\eta \sum_{j=n}^{N} E_k\, \theta'_k \{(\kappa'_{k+1} . \kappa'_{k+1}{}^H)_j - \lambda I)(\theta_k - e_k)$$

$$\Gamma_1{}^{\kappa'_k}(\theta_k, n) = \eta \sum_{j=n}^{N} E_k\, \theta'_k \,.\, \kappa'_{k+1\,j} . e_{k\,j} \quad (19)$$

Thus, the Maximum Correntropy condition described in terms of **Eigen-Space minimization** criterion is derived by us according to the ODE-MSE ensemble distribution given by authors [3] as , -

$$\left\| -\eta \sum_{j=n}^{N} E_k \, \theta'_{k+1} \left\{ \frac{\kappa'_{k+1}}{\sigma_w(k)} \right\}^{\eta_{k+1}} \{ (\kappa'_{k+1} \cdot \kappa'^{H}_{k+1})_j - \lambda I \} \right\| \leq \Omega \, (\eta^2{}_{k+1} + \eta\beta \,) \{ \Gamma(\theta_k - e_k) + 1 \}$$

Applying *Wronskian Space model* for input correlation matrix , R_{NN} , the minimization model in term of co-variance margin $\{\ddot{V}_k\}$ can be further expressed as , -

$$E_n * W \underset{N}{\leftrightarrow} (\theta_k(\Upsilon), \sigma_w(n)) = (1 - \lambda_w \, .\eta) \, W \, (\theta_k \left\{ \frac{\kappa'_{k+1}}{\sigma_w(k)} \right\}^{\eta_{k+1}} + \Omega \, (\eta^2{}_{k+1} + \eta\beta \,) \quad (20)$$

And the weight update condition according to the *"Perron-Frobenius"* condition [17][8] can be obtained as , -

$$- \lambda_w \, .\eta + \Omega \, (\eta^2{}_{k+1} \,) + \Omega \, (\eta\beta \,) \leq \lambda_w(n+1) \, .\eta \quad (21)$$

To apply maximum correntropy decision model in a Kalman-KRLS [9][13] ADALINE model, the following standard algorithm is considered . Here, ***f(∘)*** corresponds to a transformation function like Fourier-Bessel Transform as well as Huang-Hilbert Transform [14] for Gaussian Q-determinant. Upper and lower bounds are determined according to maximum MSE Probabilities as derived by authors [3] .

Initialize

$$w_0 = w(0) \;, \quad [\sigma_w(0)]^2 = [\sigma_{w_0}]^2$$

$$\widetilde{d_k(n)} = w^T{}_N(n) * h_N(n)$$

$$\dot{e}_k(n) = h_k(n) - \widetilde{d_k(n)}$$

$$w_N(n+1) = w_N(n) - \frac{1}{2} \alpha \frac{\delta \dot{e}^2{}_k}{\delta w_N} = w_N(n) + \alpha \, \dot{e}_k(n) \frac{d^T{}_n}{d_n \, d^T{}_n}$$

Iterate from

0 to → *XCorrLen* $[\eta\beta, (\mu{:}\eta)]$, *Set :* $P = \mu^T(n).\mu(n)^H$

$$L(w_N) = ln \prod_n P(h_n \mid d_k(n), w_N|) = \sum_i^M w^T{}_n f_n h_n - ln \sum_j^N e^{w^T{}_n f_n h_n}$$

Subtend / Update

$$\ddot{\alpha}(n) = \Upsilon_k(n) \left[\frac{\partial \Sigma_0^{2/\lambda}(L(w_N))}{\partial \lambda} \right] - R_{kk}{}^{-1}(n-1) \, h_{k\text{-}1}(n) . \, w_k(n)$$

$$w_N(n+1) = \lambda w_N + \lambda \left[\frac{\Sigma_0^{2/\lambda}(L(w_N)) \, h_k(n) \, \alpha(n)}{h_k{}^T(n) \, \Sigma_0^{2/\lambda}(L(w_N)) \, h_k(n) + e_k(n)} \right]$$

Approximate

$$\Sigma_0^{2/\lambda}(L(w_N)) = \lambda^2 \Sigma_0^{2/\lambda}(L(w_N)) - \ddot{V}_k + \mu_k(\mathrm{n})$$

$$\ddot{V}_k = \left[\frac{\lambda^2 \, \Sigma_0^{2/\lambda}(L(w_N)) \, h_k(n) \, h_k(n)^T \, . \, \Sigma_0^{2/\lambda}(x{\sim}n)^H}{h_k{}^T(n) \, \Sigma_0^{2/\lambda}(L(w_N)) \, h_k(n) + e_k(n)} \right]$$

Iterate and Update Cost Function (J(*))

$$\Delta(\lambda,\mu) = \sum_{n=1}^{\infty} \left(d_{x,y} \, . e^{-(d_m - W^H x_m \cdot \{d_m - W^H x_m\}^*)/2\sigma^2} \right) ;$$

$$J(\lambda,\mu) = \left[1/(2\sqrt{M}\pi\sigma^2) \right] \Delta(\lambda,\mu)$$

Determine Markovian Convergence

$$\Delta \, J(\lambda,\mu) \rightarrow \kappa'_{\theta k} \cdot e_{\theta k} = -exp \left(\frac{-(e_k{}^H) \cdot e_k}{2\sigma_w{}^2} \right) \left(\frac{e_k{}^H \sigma_w (\sigma_w - 2 \, e_k \cdot \sigma_k{}^H)}{2\sigma_w{}^4} \right)$$

Reset

$$\ddot{\alpha}(n) = \Upsilon_k(n) \left[\frac{\partial \Sigma_0^{2/\lambda}(x{\sim}n)}{\partial \lambda} \right] - R_{kk}{}^{-1}(n-1) \, h_{k\text{-}1}(n) . \, w_k(n)$$

$$\sigma_w(n+1)]^2 = [\sigma_w(n)]^2 \left(1 - \frac{h_k(n) \, / N}{h_k(n) + e_k(n) / [\sigma_w(n)]^2} \right) + \mu_k$$

$$w_N(n+1) = w_N(n) + \frac{[d_k(n) * \ddot{\alpha}(n)] + \Upsilon_k}{h_k(n) + e_k(n) \, / [\sigma_w(n)]^2}$$

4. Simulation Results

The experimental works are carried out as per the flow logic as depicted in Fig. 5. The schematic is implemented using Matlab-R/2022(a) compiler with a VeriLog assembly design.

4.1 Transmitted and Received Signal Constellation

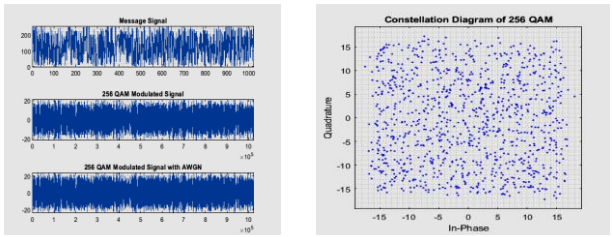

Fig. 6. *Received Constellation Scatter plot for Rake Receiver*

A 256-QAM/8-bit digital, orthogonally encoded signal is transmitted over a Rayleigh Fading channel with Active White Gaussian Noise (AWGN) margin of +10.4dB, as depicted in Fig. 6. Baud speed is set up to 2.2Mbps (IEEE-802.22x standard) [1][16] , and channel capacity is 14.2Mbps with a total channel bandwidth capacity of 15Mhz [1]. Spatial constellation plot is obtained by a rake receiver assembled with a synchronous PLL-VCO decoder.

4.2 Nyquist Cluster Estimation for 256-QAM Scatter Plot

Considering the simulation plot shown in Fig. 7, sequential sub-band cluster nodes are recursively "approximated" through

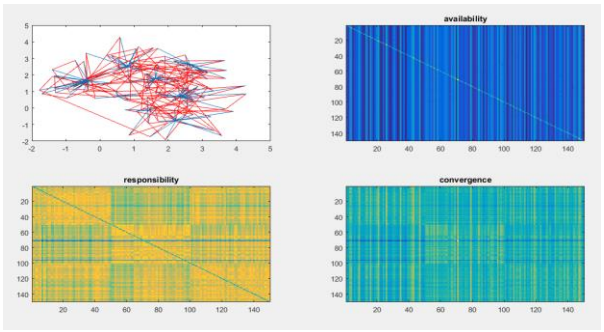

Fig. 7. *AP Clustering based on Maximum Correntropy Margins*

iterative minimization of the Euclidean Norm (Sec.III). For convenience, only an ***S/T*** windowed [16] portion is displayed.

4.3 Spectrum Ensemble and Channel Entropy Detection

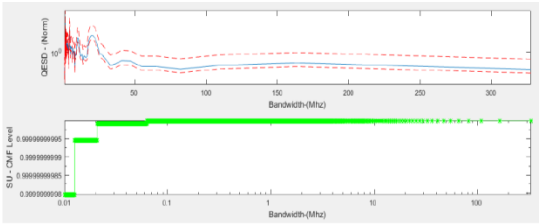

Fig. 8. *Energy Spectrum Density and Entropy Level Detection*

The Gaussian Energy Spectrum Density (ESD) extraction, as shown in Fig. 8, has been determined using a Second Order

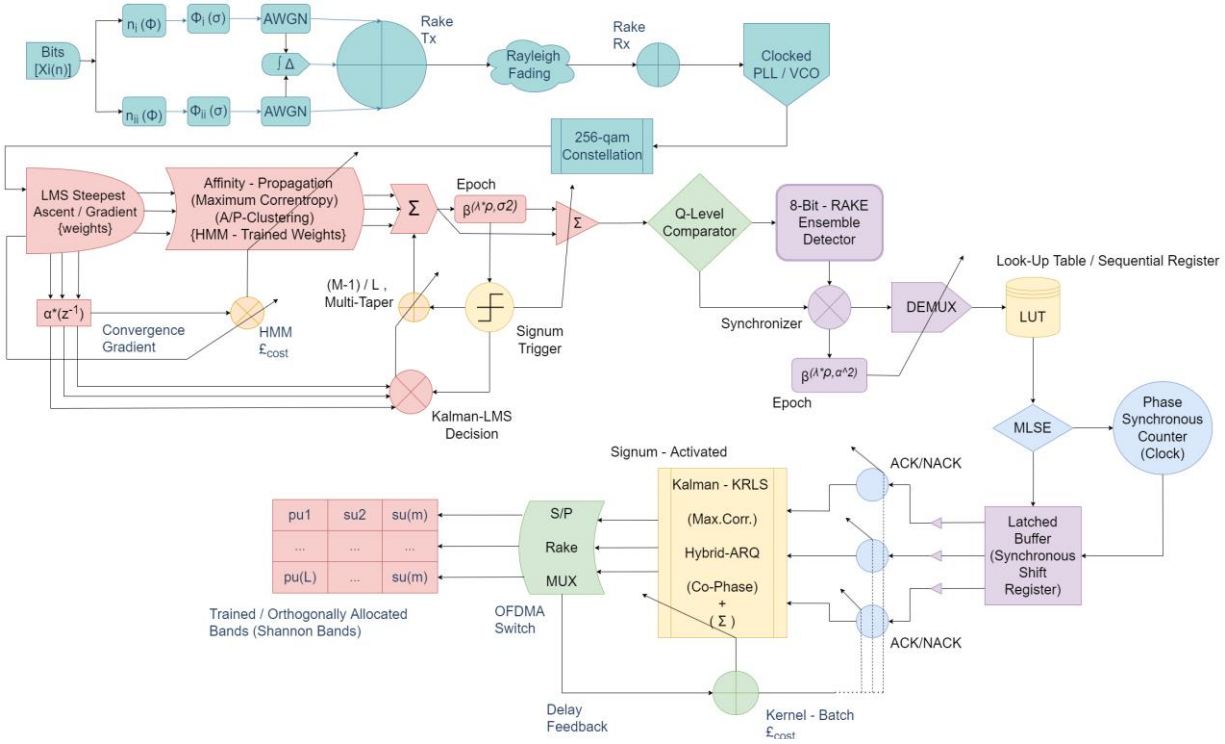

Fig. 5. *Schematic layout of Markov Trained Kalman-LMS/KRLS Adaptive Spectrum Equalizer*

Fourier-Bessel Transform sequentially traced over each identified "Nyquist clusters" as described in Section-(III). Upper bound and lower bound ensemble margins have been determined using ODE mass function limits as described by authors [3]. Thus, applying MLSE-Quantization [8][17] and Huang-Hilbert norms [14] upon the "extracted" ESD, entropy transition levels have been approximated and extracted iteratively.

4.4 Eigen-Space Minimation and Markovian Decision Nodes

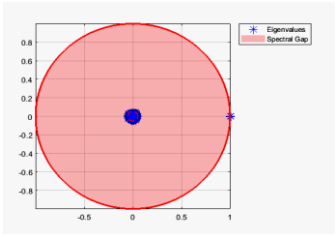

(a)

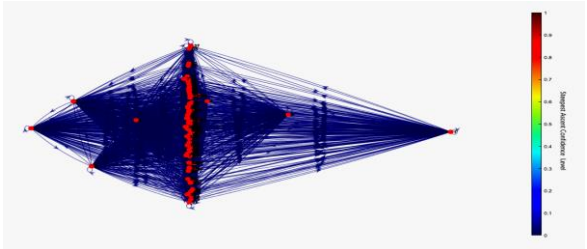

(b)

Fig. 9. *Eigen-Space Plot for Spectral Estimation (MLSE)*

Considering the simulation diagrams depicted in Fig. 9, a real time graphical visualization of the proposed ***"Perron-Frobenius"*** MLSE maximization approach [17][8] has been given as explained in Section-III. Diagram_(a) visualizes the minimum spectral dispersion condition corresponding to Eigen Spectral gaps for the determined ESD and stochastically identified CMF Gaussian Entropy levels. Diagram_(b) characterizes the conditional Central Node decision taken recursively by the Markovian SGD/SGA model for optimum channel estimation and diversity channeling as described in the next subsection.

4.5 KRLS-ARQ switching for Maximal Ratio Combination

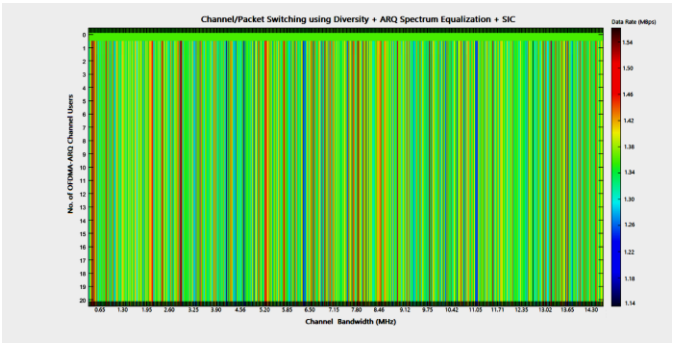

Fig. 10. *ARQ Sub-band allocation using MLSE Minimization*

Considering the weight nodal decisions taken by the Eigen-Space Entropy MLSE plot, which is used for learning and minimizing the spectral divergence in the previous subsection, the Kernelized Recursive network updates and iterates the Automatic Repeat Request (ARQ) switching delays according to the corresponding Markovian trained sequences as shown in

Fig. 10. The adaptive cost function [9][13] determined for kernel batch learning models supervises the relaying speeds for each OFDMA sub-bands (or Shannon-Bands) . The "optimum" relaying speed used for packet-buffer transmissions in each orthogonally multiplexed sub-channel is determined recursively by the KRLS-ARQ engine considering a Maximal Ratio Combination [15] condition to equalize the SNR gains while minimizing (or normalizing) the BER levels for each sub-channel. Thus, bandwidth equalization is achieved by regressively approximating the channel diversity determinants.

5. Performance Evaluation

5.1 Retransmitted Signal Improvement by ANN Equalization

Using Huang-Hilbert Transform [14] over the sequentially transmitted buffer links, we thus obtain the overall Instantaneous Bandwidth Distribution which are artificially identified for the Virtually Simulated SCADA-OFDMA Transmission Channel [1] .

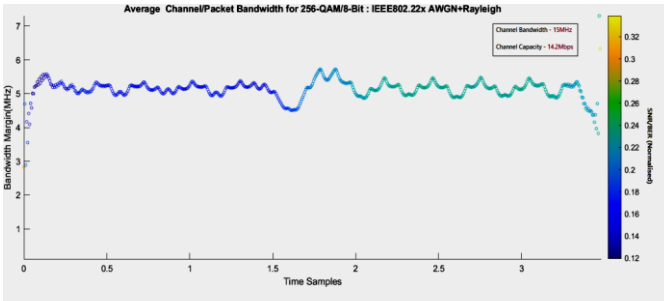

Fig. 11. *Bandwidth Distribution for Manual Transmission*

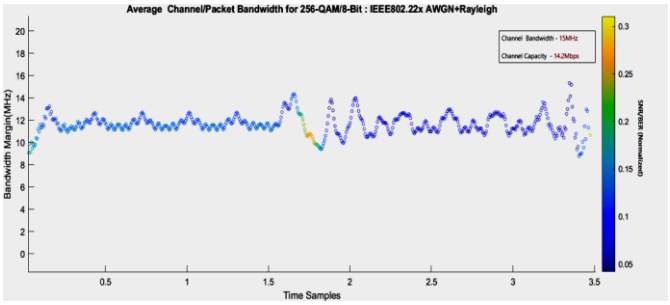

Fig. 12. *Bandwidth Distribution for Supervised Adaptive Transmission using ANN*

The given plots describe the spectrum utilization over the virtual ***IEEE-802.22x OFDMA*** adaptive channel. Fig. 11 plots the Bandwidth coverage for regular transmissions for the SCADA-DCS standard. Fig. 12 plots the same bandwidth distribution for spectrum equalized channel. We observe from comparison, that an aggregate marginal coverage of ***~94.8%*** is achieved after bandwidth equalization, as compared to the ***~48.8%*** coverage for a maximum bandwidth allotment of ***15Mhz*** with a maximum capacity of ***14.2Mbps***, with buffer speeds of ***2.8Mbps***. Thus, an absolute bandwidth improvement of nearly ***50%*** has been achieved in the allotted channel capacity. It can also be observed that normalization precision of the individual sub-channel SNR and BER ratios effect the Shannon-Band's allocation especially in a "reflexive" manner, as *over-normalizing or under-normalizing distorts* the *switching diversity decision*.

5.2 Spectrum Equalization Margins and Mean Square Errors

Considering the given plots in Fig., the individual bandwidth equalization margins with respect to the Mean Square Errors (MSE) traced over the entire tracking trajectory has been visualized. It can be observed that cascading stochastic induction in SGA/SGD based deterministic models do not hamper the regular performance of the Delta-Learning method. By stochastic gradient induction through Markov Training approach, the trained batch sizes reduce considerably which assures a large improvement in the dynamic responsiveness of conventional SGA/SGD models, as well as increasing the convergence speeds for random inputs which may or may not be causal in nature. This makes the infusion approach suitable for application in real time signal detection as well as channel allocations with observable controllability under unpredictable transmission environments.

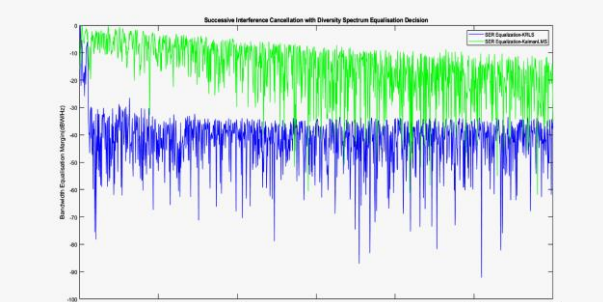

Fig. 13. *Equalization Margins for Kalman-LMS/KRLS*

Fig. 13, determines the equalization margins for Kalman-LMS ADALINE (shown in "green" fonts) as well as Kalman-KRLS ADALINE (shown in "blue" fonts). The increased regression rates for Kalman-KRLS SGD can be understood from the MSE levels during nodal transitions as given below.

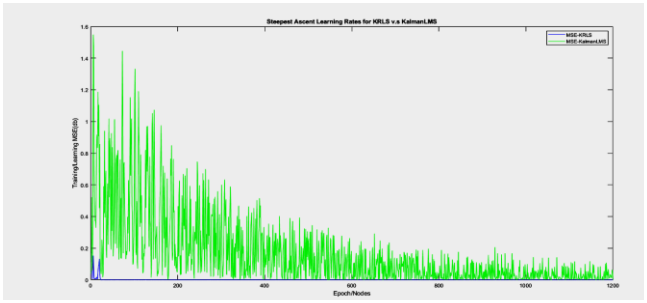

Fig. 14. *Mean Square Error (MSE) profile for Kalman-LMS/KRLS*

Fig. 14, determines the Learning Accuracies in terms of MSE convergence patterns for Kalman-LMS ADALINE (shown in "green" fonts) as well as Kalman-KRLS (shown in "blue" fonts). We can observe that a considerably high degree of *over-learning* and *over-training* situation can be seen for KRLS-SGD in comparison to the ergodically transient convergence pattern observed for Kalman-LMS SGD. Thus, dynamic adaptability is maintained in cluster detection while discreteness in the regression pattern can be ascertained for

diversity allocation, provided the cost functions are iterated properly with a proper selection of minimization rates. Improper selection of minimization rates can severely destabilize the tracking performances as well.

6. Conclusion

In this paper, we have implemented and simulated a novel Stochastic Markov infusion concept over a Kalman optimized Steepest Gradient Ascent / Descent based Adaptive Artificial Neural Network to virtually implement a network resource allocation based operation in a SCADA-DWWAN based transmission standard (IEEE-802.22x) using OSI-4.0 Architecture. Learning performances have been observed with respect to the improvement in bandwidth allocation though spectrum equalization approach over an OFDMA-ARQ based adaptive multiplexed channel. Results show dynamic adaptability, improved efficiency as well as large reduction of the training complexity through stochastic infusion in decisive ADALINE approaches.

Acknowledgement

The author would like to confer his solemn gratitude to the Department of Electronics and Communication Engineering (ECE), under Gauhati University for providing technical support and guidance towards the completion of this simulation based project.

References

[1] IEEE Std C37.1TM-20017, "*IEEE Standard for SCADA and Automation Systems*" 2018R-TM @ IEEE Power and Energy Society, IEEE, USA, 2018, pp. 19-21.

[2] Li, Qiang & Shen, Dong & Wang, Fei. (2016) , *"MQAM Modulation Recognition Based on AP Clustering Method", MATEC Web of Conferences. 44. 01002. 10.1051/matecconf/20164401002.DOI:10.1051/matecconf/20164401002 PubINC:January 2016, MATEC Web of Conferences 44:0100*

[3] G. G. Yin and V. Krishnamurthy, "LMS algorithms for tracking slow Markov chains with applications to hidden Markov estimation and adaptive multiuser detection," in IEEE Transactions on Information Theory, vol. 51, no. 7, pp. 2475-2490, July 2005, doi: 10.1109/TIT.2005.850075.

[4] X. Liu, M. Yin, J. Luo and W. Chen, "An improved affinity propagation clustering algorithm for large-scale data sets," 2013 Ninth International Conference on Natural Computation (ICNC), 2013, pp. 894-899, doi: 10.1109/ICNC.2013.6818103.

[5] Imen Nasr , Sofiane Cherif , Published in: 2012 IEEE Vehicular Technology Conference (VTC Fall) Date of Conference: 3-6 Sept. 2012 Date Added to IEEE *Xplore*: 31 December 2012 ISBN/ISSN Information: INSPEC Accession Number: 13226663 DOI: 10.1109/VTCFall.2012.6399369

Pp.: "A Novel Adaptive Fusion Scheme for Cooperative Spectrum Sensing" Publisher: IEEE Conference Location: Quebec City, QC, Canada

[6] P. A. C. Lopes and J. B. Gerald, *"New Normalized LMS Algorithms Based on the Kalman Filter" , 2007 IEEE International Symposium on Circuits and Systems*, 2007, pp. 117-120, DOI:10.1109/ISCAS.2007.378235. Published in: 2007 IEEE International Symposium on Circuits and Systems INSPEC Accession Number: 9538973 DOI: 10.1109/ISCAS.2007.378235 Print ISBN : 1-4244-0920-9 CD:1-4244-0921-7 Print ISSN: 0271-4302 Electronic ISSN: 2158-1525

[7] Jian Hua.Lu, K.B Letaif, M.L Liou, J.C.I-Chuang, *"M-PSK and M-QAM BER computation using signal-space concepts in OFDMA Channel Switched ARQ"* Published in: IEEE Transactions on Communications (Volume: 47, Issue: 2, Feb 2012) INSPEC Accession Number: 6212385 DOI: 10.1109/26.752121 Publisher : IEEE (RC)

[8] *Amit Baghel , Monika Kumari , Published in: 2020 IEEE International Conference for Innovation in Technology (INOCON) Date of Conference: 6-8 Nov. 2020 Date Added to IEEE Xplore: 01 January 2021 ISBN Information: INSPEC_Accession Number: 20334148 DOI: 10.1109/INOCON50539.2020.9298447 Publisher: IEEE Conference Location: Bangaluru, India Pp. : "Spectrum Sensing using Analysis of Variance, Eigen, and Energy (ANOVEE)" .*

[9] Façanha, T.S., Barreto, G.A. & Costa Filho, J.T. A Novel Kalman Filter Formulation for Improving Tracking Performance of the Extended Kernel RLS. *Circuits Syst Signal Process, Springer Pub*. 40, 1397–1419 (2021). https://doi.org/10.1007/s00034-020-01533-4

[10] K. N. Pappi, A. S. Lioumpas and G. K. Karagiannidis, "θ-QAM: A parametric quadrature amplitude modulation family and its performance in AWGN and fading channels," in IEEE Transactions on Communications, vol. 58, no. 4, pp. 1014-1019, April 2010, doi: 10.1109/TCOMM.2010.04.080552.

[11] S. Saraç and Ü. Aygölü, "An ARQ-based protocol for cooperative spectrum sharing in underlay cognitive radio," 2016 24th Signal Processing and Communication Application Conference (SIU), 2016, pp. 405-408, doi: 10.1109/SIU.2016.7495763.

[12] Y. Chen, H. C. Lee, J. You and S. Wei, "Less Complexity Successive Interference Cancellation for OFDM System," 2007 IEEE 18th International Symposium on Personal, Indoor and Mobile Radio Communications, 2007, pp. 1-5, doi: 10.1109/PIMRC.2007.4394648.

[13] Aquino, M.B.L., F. Guimarães, J.P., Linhares, L.L.S. *et al.* Performance evaluation of the maximum complex correntropy criterion with adaptive kernel width update. *EURASIPJ. Adv. Signal Process.* **2019,** 53(2019). Springer Open. EURASIP https://doi.org/10.1186/s13634-019-0652-2

[14] Y. Liu, H. An and S. Bian, "Hilbert-Huang Transform and the Application," 2020 IEEE International Conference on Artificial Intelligence and Information Systems (ICAIIS), 2020, pp. 534-539, doi: 10.1109/ICAIIS49377.2020.9194944.

[15] T. Kumagai, M. Mizoguchi, T. Onizawa, H. Takanashi and M. Morikura, "A maximal ratio combining frequency diversity ARQ scheme for OFDM signals," Ninth IEEE International Symposium on Personal, Indoor and Mobile Radio Communications (Cat. No.98TH8361), 1998, pp. 528-532 vol.2, doi: 10.1109/PIMRC.1998.734257.

[16] Solanki, Surendra & Dehalwar, Vasudev & Choudhary, Jaytrilok. (2021). Deep Learning for Spectrum Sensing in Cognitive Radio. Symmetry. 13. 147. 10.3390/sym13010147.

[17] S. U. Pillai, T. Suel and Seunghun Cha, "The Perron-Frobenius theorem: some of its applications," in IEEE Signal Processing Magazine, vol. 22, no. 2, pp. 62-75, March 2005, doi: 10.1109/MSP.2005.1406483.